AD-A115 611 SRI INTERNATIONAL MENLO PARK CA F/G 17/2.1
HF RADIONOISE MODELS FOR SEVERELY DISTURBED PROPAGATION ENVIRON--ETC(U)
MAR 81 G H PRICE, V E HATFIELD DNA001-80-C-0253
UNCLASSIFIED DNA-5734T NL

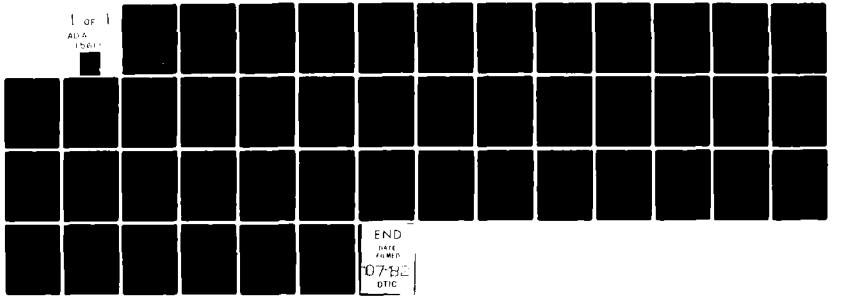

AD-E300 993

(12)

DNA 5734T

AD A115611

HF RADIO-NOISE MODELS FOR SEVERELY DISTURBED PROPAGATION ENVIRONMENTS

Gary H. Price

V. Elaine Hatfield

SRI International
333 Ravenswood Avenue
Menlo Park, California 94025

31 March 1981

Topical Report for Period 15 September 1980—31 March 1981

CONTRACT No. DNA 001-80-C-0253

APPROVED FOR PUBLIC RELEASE; DISTRIBUTION UNLIMITED.

THIS WORK SPONSORED BY THE DEFENSE NUCLEAR AGENCY
UNDER RDT&E RMSS CODE B322080464 S99QAXHB05313 H2590D.

DTIC FILE COPY

Prepared for
Director
DEFENSE NUCLEAR AGENCY
Washington, D. C. 20305

82 05 18 097

Destroy this report when it is no longer needed. Do not return to sender.

PLEASE NOTIFY THE DEFENSE NUCLEAR AGENCY, ATTN: STTI, WASHINGTON, D.C. 20305, IF YOUR ADDRESS IS INCORRECT, IF YOU WISH TO BE DELETED FROM THE DISTRIBUTION LIST, OR IF THE ADDRESSEE IS NO LONGER EMPLOYED BY YOUR ORGANIZATION.

UNCLASSIFIED

SECURITY CLASSIFICATION OF THIS PAGE (When Data Entered)

REPORT DOCUMENTATION PAGE		READ INSTRUCTIONS BEFORE COMPLETING FORM
1. REPORT NUMBER DNA 5734T	2. GOVT ACCESSION NO. AD-A115 611	3. RECIPIENT'S CATALOG NUMBER
4. TITLE (and Subtitle) HF RADIO-NOISE MODELS FOR SEVERELY DISTURBED PROPAGATION ENVIRONMENTS		5. TYPE OF REPORT & PERIOD COVERED Topical Report for Period 15 Sep 80—31 Mar 81 6. PERFORMING ORG. REPORT NUMBER SRI Project 1856
7. AUTHOR(s) Gary H. Price V. Elaine Hatfield		8. CONTRACT OR GRANT NUMBER(s) DNA 001-80-C-0253
9. PERFORMING ORGANIZATION NAME AND ADDRESS SRI International 333 Ravenswood Ave Menlo Park, California 94025		10. PROGRAM ELEMENT, PROJECT, TASK AREA & WORK UNIT NUMBERS Subtask S99QAXHB053-13
11. CONTROLLING OFFICE NAME AND ADDRESS Director Defense Nuclear Agency Washington, D.C. 20305		12. REPORT DATE 31 March 1981 13. NUMBER OF PAGES 46
14. MONITORING AGENCY NAME & ADDRESS(if different from Controlling Office)		15. SECURITY CLASS (of this report) UNCLASSIFIED 15a. DECLASSIFICATION/DOWNGRADING SCHEDULE N/A since UNCLASSIFIED

16. DISTRIBUTION STATEMENT (of this Report)

Approved for public release; distribution unlimited.

17. DISTRIBUTION STATEMENT (of the abstract entered in Block 20, if different from Report)

18. SUPPLEMENTARY NOTES

This work sponsored by the Defense Nuclear Agency under RDT&E RMSS Code B322080464 S99QAXHB05313 H2590D.

19. KEY WORDS (Continue on reverse side if necessary and identify by block number)

Nuclear Environments
Atmospheric Noise
Cosmic Noise
Local Noise
HF Radio Noise

20. ABSTRACT (Continue on reverse side if necessary and identify by block number)

Models and sample results are given for the natural HF radio-noise environment under conditions of severe disturbance to HF sky-wave propagation, such as might be produced by the detonation of numbers of high-altitude nuclear explosions in a major attack. Both local and remote atmospheric-noise sources are treated, and the effects on cosmic noise and atmospheric noise of changes in the F-region critical frequency are included.

DD FORM 1 JAN 73 1473 EDITION OF 1 NOV 65 IS OBSOLETE

UNCLASSIFIED

SECURITY CLASSIFICATION OF THIS PAGE (When Data Entered)

TABLE OF CONTENTS

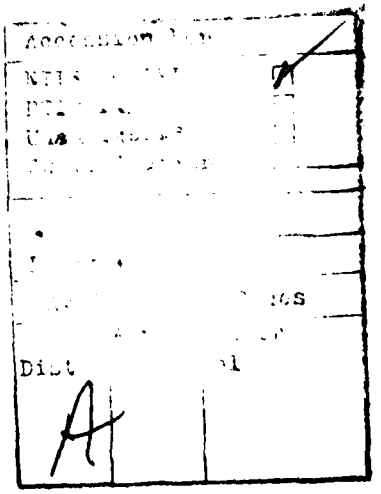

LIST OF ILLUSTRATIONS

LIST OF TABLES

I INTRODUCTION AND SUMMARY

Evaluation of the performance of HF radio-communication systems requires that certain basic characteristics of both the signal and the noise with which it is received be known. Propagation plays a major role in determining these characteristics. Consequently, pronounced changes in HF propagation behavior produced by high-altitude nuclear detonations can affect the performance of a HF communication system. Complex computer codes* have been developed to assess the impact of such propagation changes on signal characteristics. Applying these codes to HF radio noise is, however, computationally awkward because of the wide geographic distribution and variability of natural noise sources. This report (the second of two† prepared for the Defense Nuclear Agency) describes a model that avoids this difficulty under conditions of sufficiently severe and widespread propagation attenuation, such as would result if several high-altitude "blackout" detonations were included in a nuclear attack.

Price and Smith[1] outlined a simplified HF noise model that could be applied to severely disturbed propagation environments, and discussed the approximations through which the model was developed. A finished implementation of the model was, however, not presented; we complete this work in Section II of this report. The data base used to evaluate the empirical parameters through which lightning is related in the model to equivalent noise-source temperature has also been expanded, improving the accuracy of the values obtained for these parameters. Additionally,

*E.g., NUCOM

†The first report is Price and Smith.[1] All references are listed at the end of this report.

the model has been used to calculate the effects on the noise of a disturbed environment, similar to that found in the vicinity of Johnston Island following the STAR FISH detonation. Comparison of the model results with HF noise measurements made in Hawaii shows satisfactory consistency (the ionospheric disturbance produced by STAR FISH was not sufficiently uniform over a wide area so that the model could be strictly applied to these data).

A treatment of locally produced atmospheric radio noise is presented in Section III. This noise contribution, which is unaffected by high-altitude detonations, is not properly dealt with in the simpler model discussed in Section II. The model departs from the Rayleigh amplitude-distribution function (implicitly assumed in the simpler model) at the low-probability/high-amplitude extreme of the distribution when local noise is included. These high amplitudes occur more frequently with the improved model (although still infrequently) than is predicted by the Rayleigh distribution.

The simple model presented in Section II can be readily incorporated into current HF nuclear-effects propagation-prediction codes; such inclusion is recommended. The local-noise model discussed in Section III is not, however, suitable for incorporation into these codes in its present form. We recommend that this model first be reduced, insofar as possible, to table form, with the tables calculated using an improved numerical version of the present implementation. Finally, extension of the methodology developed to treat local noise to provide a unified treatment of both local and remote noise is also recommended. Such extension, along the lines outlined in Section III.B, will improve the description provided by the overall model of atmospheric noise amplitude statistics in disturbed propagation environments. Finally, experiments to validate the local-noise model, and its generalization, should be undertaken because the experimental data upon which the model is based are, as is noted in Section III of this report, weak in several particulars.

II TESTING, CHECKING, AND EVALUATING THE BASIC NOISE MODEL

A. Introduction

A basic model for natural HF noise in severely disturbed propagation environments was described in Price and Smith.[1] The task reported on here is to review this model, including the improvements that have been implemented in accordance with the recommendations made in Price and Smith.[1] In this process, we have accomplished the following:

(a) Checked the physical parameters and confirmed that they are correctly included.

(b) Expanded the data base used to derive the values of empirical parameters, thereby improving their accuracy.

(c) Applied the model to demonstrate its performance in its intended environment.

The physical parameters involved in the model were indicated in Price and Smith,[1] but simple averages and only rough estimates were used to establish the functional relationship between thunderstorm activity and equivalent noise temperature. For ease in making this relationship more precise, a computer program representing the model has been written on the SRI Prime computer. Several changes from the earlier version have been included. The dependence of equivalent source temperature on elevation angle is now included in the lightning integral, and an analytic representation of the normal D region has been added.

The data base for deriving the empirical relationship between thunderstorm activity and equivalent noise temperature has been expanded to include nine additional cases. A larger, more diverse data base can probably improve the model further, but care must be exercised in its selection because only in certain cases is the model applicable to the normal environment. A sample case in a nuclear environment was run on the program to show how the model will work.

Section II.B describes the equations that are used in the current version of the basic model. Section II.C describes the computation of the empirical coefficients and evaluates them. Section II.D describes and evaluates the results of a test case run for a nuclear environment.

B. Model Equations

The basic model was derived in Price and Smith.[1] This section explains in detail some portions of the model that were only outlined in the earlier report. This model is only for severely disturbed conditions, and is not a general model. The severely disturbed environment can be described as one in which D-region losses are high over a large region. This condition can be produced in a nuclear environment if high-altitude radioactive debris is widespread, extending in all directions for a considerable distance (thousands of kilometers) from the receiver. More precisely, the limitations imposed are:

(1) Only sources relatively near (within a few thousand kilometers of) the receiver are significant.

(2) Lightning activity in this source area is (statistically) the same as that in the immediate vicinity of the receiver.

(3) Sky-wave propagation characteristics are uniform over this region, with high losses; therefore, only one-hop paths are significant.

The general equation for antenna noise temperature, $T_A(f)$, presented in Price and Smith[1] (page 13) can be written:

$$T_A(f) = \frac{\int_0^{\pi/2} d\theta \sin\theta \int_0^{2\pi} d\phi\, p(\theta, \phi, f) \left[1 + R^2(\theta, f)\right] T_s(\theta, f)}{\int_0^{\pi/2} d\theta \sin\theta \int_0^{2\pi} d\phi\, p(\theta, \phi, f) \left[1 + R^2(\theta, f)\right]} \qquad (1)$$

where

f = operating frequency (MHz)

ϕ = azimuthal angle

Θ = zenith angle

$p(\Theta, \phi, f)$ = receiver antenna power gain pattern

$T_s(\Theta, f)$ = apparent sky temperature

$R(\Theta, f)$ = ground reflection loss (this parameter was omitted in Price and Smith.[1])

The apparent sky temperature, $T_s(\Theta, f)$, is the source term in the noise model. It is described in terms of the most important noise sources, lightning and cosmic processes. As a function of zenith angle, Θ, these sources are mutually exclusive. The switch from one source to the other occurs as the path of the arriving noise shifts from ionospheric reflection to penetration. The zenith angle for the switch is calculated:

$$\Theta_c(f) = \sin^{-1}\left\{\frac{r_e}{r_p}\left[1 - \left(\frac{f_c}{f}\right)^2\right]^{1/2}\right\} \qquad (2)$$

where

r_e = radius of the earth

r_p = distance from center of earth to the peak of the ionospheric electron density profile

f_c = critical frequency of the ionosphere.

The galactic noise is received from the region $\Theta = 0$ to Θ_c, and the atmospheric noise is received in the region $\Theta = \Theta_c$ to $\pi/2$. The apparent sky temperature from either source is reduced by propagation losses through the absorbing region, and the absorbing medium responsible for them itself radiates thermally. These phenomena can be represented mathematically as follows:

(1) Sky Temperature Due to Lightning Source

for $\Theta = \Theta_c(f)$ to $\pi/2$

$$T_s(\Theta, f) = T_L(\Theta, f)\left[(1 + R^2(\Theta, f)\right]$$

$$\times \left(\frac{10^{-2L_{v_o}(f) \sec i/20} + 10^{-2L_{v_x}(f) \sec i/20}}{2} \right)$$

$$+ T_r\left[1 - \left(\frac{10^{-2L_{v_o}(f) \sec i/20} + 10^{-2L_{v_x}(f) \sec i/20}}{2} \right)\right] \qquad (3)$$

where

$L_{v_o}(f)$ = one-way vertical absorption for frequency, f, on ordinary ray

$L_{v_x}(f)$ = one-way vertical absorption for frequency, f, on extraordinary ray

i = ray incidence angle to the ionospheric layer at the maximum absorbing height (D region approximately 70 km)

T_r = D-region radiative temperature (283 K) (note change of notation from Price and Smith[1])

$T_L(\Theta, f)$ = lightning-noise source temperature

$= \alpha_0 f^{-\alpha_1} \sigma_h \sec \Theta$

σ_h = lightning flashes/km^2/hour

$= (0.03\ T_m + 0.009\ T_m^{\cdot 2})/720^* \times TA_h \times 24/100$

(Cianos and Pierce[2])

*Hours per month.

where

T_m = thunderstorm days per month (as given in Reference 3.)

TA_h = thunderstorm activity per hour (as given in Cianos and Pierce[2].)

α_0, α_1 = empirical constants derived in next section.

(2) Sky Temperature Due to Galactic Sources

for $\Theta = 0$ to $\Theta_c(f)$

$$T_s(\Theta, f) = T_c(f) \left(\frac{10^{-L_{v_o}(f) \sec i/20} + 10^{-L_{v_x}(f) \sec i/20}}{2} \right)$$

$$+ T_R \left[1 - \left(\frac{10^{-L_{v_o}(f) \sec i/20} + 10^{-L_{v_x}(f) \sec i/20}}{} \right) \right] \qquad (4)$$

where

$T_c(f) = 100\ \lambda^{2.3}$ (CCIR[4])

λ = wavelength in meters = 300/f.

The absorption losses $L_{v_o}(f) \sec i$ and $L_{v_x}(f) \sec i$ are doubled for lightning to account for the ascending and descending portions of the path; for cosmic noise, these losses appear once, because the ray path only makes one pass through the absorbing region.

C. Calculation of the Coefficients for Computing the Sky Temperature Due to Lightning

Empirical coefficients for the sky-temperature model were computed by using data taken in a normal environment, with the requirement that the data must also satisfy the limitations listed in Section II.B. These conditions are satisfied if ambient propagation losses are sufficiently high. A summer month, July, was chosen and appropriate data values of $F_A(f)$ from CCIR[4] were found for four separate cases. Table 1 lists the data used. The CCIR data base was collected between 1957 and 1961. An average SSN of 140 was estimated for that period. $F_A(f) = 10 \log T_A(f)/T_0$ where $T_0 = 288$ K.

The empirical coefficients $\alpha_o = 5.27 \times 10^{15}$ and $\alpha_1 = -7.11$ in the functional relationship $T_L(\Theta, f) = \alpha_0 f^{-\alpha_1} \sigma_h \sec \Theta$ were derived by substituting the parameters from Table 1 into Eq. (1) and solving for α_0 and α_1 by least squares. The relationship is linear on a log scale. Figure 1 shows a plot of the data $\alpha = \alpha_0 f^{-\alpha_1}$ as a function of frequency, f, together with the least squares linear fit to the data for the four cases. The standard error for this limited data set is 0.229 on the log scale.

A check was made to see if the daily and hourly variation in thunderstorm activity over the four cases fitted, has contributed to the quality of the fit. Elimination of σ_h from the computation increased the standard error of the fit by 14 percent--a significant change given the general similarity of the cases.

D. A Comparison of Model Results with Observed Disturbed-Environment Noise

The STAR FISH high-altitude nuclear detonation over Johnston Island on 9 July 1962, provides an interesting example with which to compare our model. Herman[7] reported that the 5-MHz radio noise measured at Kekaha, Hawaii was about 12 dB below normal level at one hour following STAR FISH, with a smaller decrease at higher frequencies. Data also

Table 1

PARAMETERS USED IN DERIVING THE EMPIRICAL RELATIONSHIP BETWEEN THUNDERSTORM ACTIVITY AND EQUIVALENT SKY-NOISE TEMPERATURE

Case No.	F_A^* (dB)	Thunderstorm		f (MHz)	f_H § (MHz)	Receiver		f_0F_2 ** (MHz)	HF_2 ** (km)	UT	Local Time	Ground Loss§
		Days Per Month +	Activity Per Hour ‡ (percent)			Latitude (Degrees North)	Longitude (Degrees West)					
1	40.0	8	5.0	5.	1.5	40	90	7.0	352	2000	1400	Poor earth
	37.5	8	5.0	10.	1.5	40	90	7.0	352	2000	1400	Poor earth
	36.0	8	5.0	15.	1.5	40	90	7.0	352	2000	1400	Poor earth
2	55.0	8	8.5	5.	1.5	40	90	6.9	333	2200	1800	Poor earth
	47.5	8	8.5	10.	1.5	40	90	6.9	333	2200	1800	Poor earth
	42.5	8	8.5	15.	1.5	40	90	6.9	333	2200	1800	Poor earth
3	47.5	12	6.0	5.	1.1	12	85	12.5	382	2000	1400	Poor earth
	41.0	12	6.0	10.	1.1	12	85	12.5	382	2000	1400	Poor earth
	38.5	12	6.0	15.	1.1	12	85	12.5	382	2000	1400	Poor earth
4	55.0	12	7.5	5.	1.1	12	85	11.8	377	2200	1800	Poor earth
	47.5	12	7.5	10.	1.1	12	85	11.8	377	2200	1800	Poor earth
	42.5	12	7.5	15.	1.1	12	85	11.8	377	2200	1800	Poor earth

*CCIR[4]

+WMO[3]

‡Cianos and Pierce[2]

§Davies[5]

**Barghausen[6]

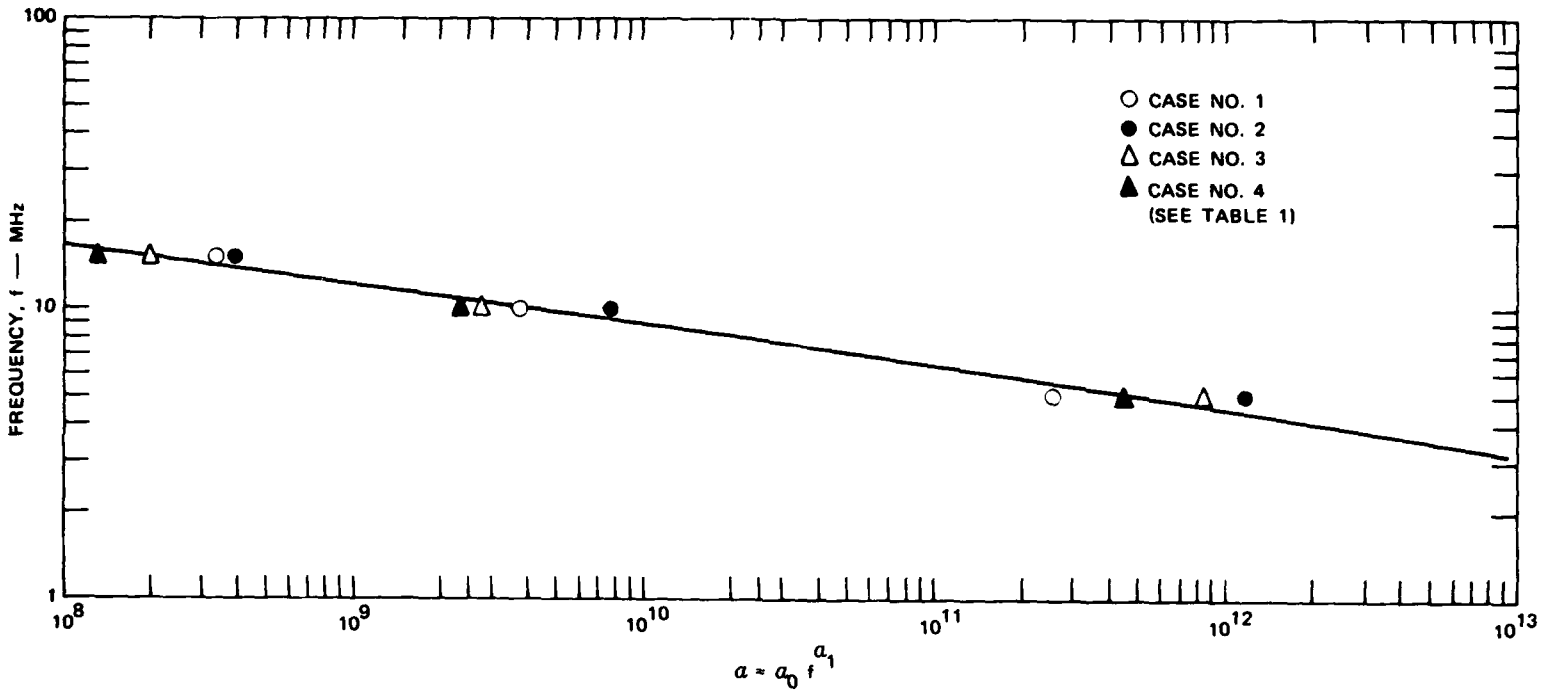

FIGURE 1 EMPIRICAL FIT FOR FREQUENCY DEPENDENCE OF THUNDERSTORM TEMPERATURE FUNCTION

are available* from Johnston Island for vertical absorption and for F-region critical frequency variations following STAR FISH. These data have been used as input to our noise model to obtain the expected noise level at Johnston Island at one hour after the shot. The results of this calculation are summarized in Table 2, along with the values of other parameters that have been input to the calculation.

If the D-region ionization produced by STAR FISH were sufficiently widespread, the noise reduction calculated for Johnston Island and the noise reduction observed at Kekaha could be expected to be similar. This, however, was not the case; the calculated noise reduction at Johnston Island caused by the detonation exceeds that observed at Kekaha by a considerable margin. This result is consistent with Herman's[7] analysis of the noise data, in which he finds thunderstorm activity in the Americas, eastward of Kekaha, to be a major source of the noise received there. The propagation path of this noise was little affected (at one hour) by the STAR FISH debris, which, at this time, remained largely westward of Kekaha.

*Unpublished DNA reports.

Table 2

SUMMARY OF RESULTS FROM AND INPUT TO COMPUTATION OF JOHNSTON ISLAND HF NOISE ENVIRONMENT AT ONE HOUR FOLLOWING STAR FISH

Frequency (MHz)	$F_a(f)$		f_0F_2 (MHz)	Increased Absorption above Normal at 30 MHz (dB)	UT	Location		SSN	Thunderstorm	
	Disturbed (dB)	Normal (dB)				Latitude (Degrees N)	Longitude (Degrees W)		Days per Month	Activity per Hour
5	-0.1	48	2.5	2	1000	16.7	169.5	40	1	4
10	2.6	39	2.5	2	1000	16.7	169.5	40	1	4
15	9.0	27	2.5	2	1000	16.7	169.5	40	1	4

III NOISE OF LOCAL ORIGIN

Noise of local origin, that is, noise produced within line-of-sight (or ground-wave) range of the receiving antenna, is unaffected by the changes in ionospheric propagation loss with which we have largely been concerned in Section II. A lightning discharge at such close distances is, however, a relatively rare event. For example, a mean rate of occurrence of ten flashes per square kilometer per month, a value representative of regions of moderately high thunderstorm activity, implies only about a 50-percent probability of a flash (mean duration 0.5 s) being in progress within a 250-km range (line-of-sight for a source at 5-km altitude and a receiving antenna at ground level) at any given time. This sporadicity of occurrence must be accounted for in modeling noise of local origin.

A. Isolated Flashes

The problem of describing locally-produced noise can be divided into two parts. The first of these is to define the probability that a local lightning flash is in progress, and the second is to characterize the noise given that a flash is, or is not, in progress. Statistically, if p(E) represents the probability density distribution for the noise field envelope amplitude at the receiving antenna, then

$$p(E) = p(E|\text{no flash})\ P(\text{no flash}) + p(E|\text{flash})\ P(\text{flash}) \quad . \qquad (5)$$

In the absence of a local flash, the noise will be considered Gaussian within the bandwidths of interest, with a variance determined by the effective antenna temperature, T. Thus, we have

$$p(E|\text{no flash}) = \frac{E}{\sigma_0^2} \exp\left(-\frac{E^2}{2\sigma_0^2}\right) \qquad (6)$$

where the variance, σ_0^2, is given by CCIR[4] as

$$\sigma_0^2 = 2.82 \times 10^{-34} f^2 B \frac{\bar{T}}{T_0} \quad (V/m)^2 \tag{7}$$

if both the receiver bandwidth, B, and frequency, f, are measured in Hertz, and the reference temperature, T_0, is 288 K. This noise component represents the aggregate of more distant lightning flashes or cosmic noise (or both) treated in Section II; the effective antenna temperature, T, is defined as $T_A(f)$.

Regarding the noise emitted by local lightning flashes, relatively few studies have addressed the statistical characteristics of the HF radio emissions from individual flashes. Oetzel and Pierce[8] characterize this noise as a quasi-continuous burst of radiation that continues over the duration of the flash--typically some hundreds of milliseconds. Horner[9] offers a similar description and summarizes, in terms of mean spectral amplitude as a function of frequency, various measurements of source strength. These data are reproduced in Figure 2.

Although significant fluctuations in radiated power occur over the duration of a flash (most notably the cessation of HF emission for some milliseconds following a return stroke of a flash to ground[8]), it seems adequate for our purposes to treat the HF radiation as a statistically uniform process throughout the flash. The noise also will be considered Gaussian, or "white," over bandwidths of interest, although there is some evidence[10] for occasional isolated, broadband spikes of HF radiation that may not be well represented by such a model.

The randomness of flash location, which produces at the receiving antenna a randomness in the mean power received during a flash, must also be considered. The noise power incident on the antenna is described by the variance, σ_1^2, of the noise-amplitude distribution. Generally, σ_1^2 is a function of the distance between source and receiver. Because this distance is a random variable, so is σ_1^2. The net noise received during a flash is the sum of the noise background and that produced by the flash.

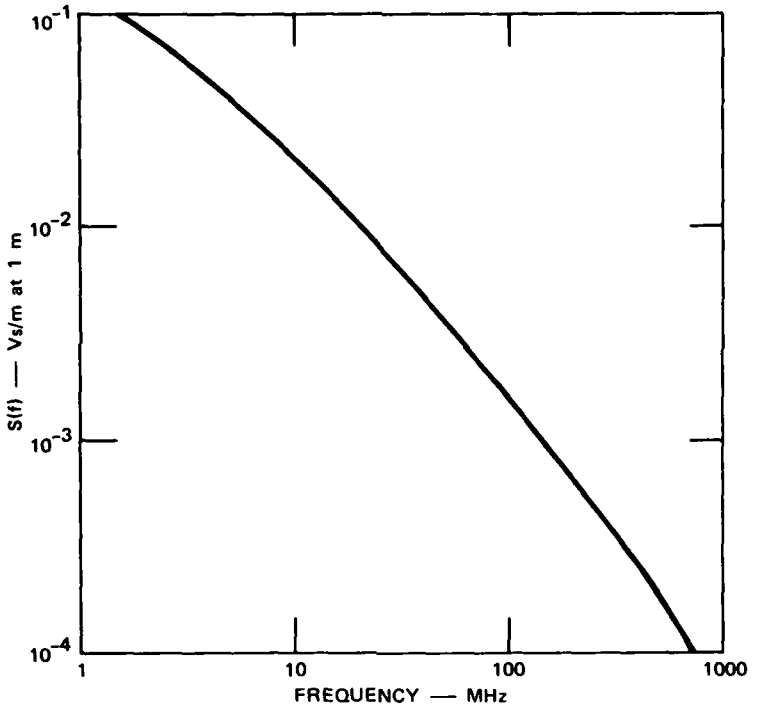

FIGURE 2 HF/VHF SPECTRUM OF LIGHTNING ATMOSPHERICS (AFTER HORNER[9])

Both of these noise components are modeled as Gaussian random variables, so their sum is also Gaussian with a variance, σ^2, that is the sum of those for the two components:

$$\sigma^2 = \sigma_0^2 + \sigma_1^2 \quad . \tag{8}$$

The probability density function for the net noise incident on the antenna during a flash can now be written as an integration over the distribution of σ^2. We have

$$p(E|\text{flash}) = \int d\sigma^2 \; p(\sigma^2) \; p(E|\text{flash}, \sigma^2) \tag{9}$$

where

$$p(E|\text{flash},\ \sigma^2) = \frac{E}{\sigma^2} \exp\left(-\frac{E^2}{2\sigma^2}\right) \quad . \tag{10}$$

The probability density function for σ^2, $p(\sigma^2)$, is derived from that for σ_1^2:

$$p(\sigma^2) = p(\sigma_1^2 = \sigma^2 - \sigma_0^2) \quad . \tag{11}$$

The times of occurrence of lightning flashes are taken to be uncorrelated and (statistically) distributed uniformly over time in the short term. (The mean flash rate is, however, allowed to vary diurnally and seasonally.) Thus, the probability of occurrence of N flashes within some time interval, τ, is given by the Poisson distribution:

$$P(N,\tau) = \frac{(\bar{n}\tau)^N \exp(-\bar{n}\tau)}{N!} \tag{12}$$

where $\bar{n}$ is the mean flash rate. If τ is set equal to the mean duration of a flash, then it can be shown that $P(N,\tau)$ also is the probability that N flashes are in progress simultaneously; $P(0,\tau)$ and $P(1,\tau)$ will be required for evaluation of Eq. (5) from Eq. (12).

$$P(\text{no flash}) = P(0,\tau) = \exp(-\bar{n}\tau) \quad , \tag{13a}$$

$$P(\text{flash}) = P(1,\tau) = \bar{n}\tau \exp(-\bar{n}\tau) \quad . \tag{13b}$$

Assume for the moment that the probability of more than one local flash in progress simultaneously in a region of low thunderstorm activity is negligible. Flash rates in regions of high thunderstorm activity are, however, sufficiently great that extension of the model to treat overlapping flashes is desirable. Such extension, although analytically straightforward, is numerically taxing. It will be discussed in Section III.B.

To obtain the probability-density function for the envelope amplitude of the incident noise, Eq. (5) must be evaluated. If we insert into this equation, the expressions from Eqs. (6), (9), (10), (11) and (13), developed for its component parts, we have

$$p(E) = \exp(-\bar{n}\tau)\,\frac{E}{\sigma_0^2}\exp\left(-\frac{E^2}{2\sigma_0^2}\right)$$

$$+\,\bar{n}\tau\,\exp(-\bar{n}\tau)\int_{\sigma_0^2}^{\infty} d\sigma^2\; p\left(\sigma_1^2 = \sigma^2 - \sigma_0^2\right)\frac{E}{\sigma^2}\exp\left(-\frac{E^2}{2\sigma^2}\right) \quad . \qquad (14)$$

Eq. (14) can be easily integrated with respect to E to obtain the probability-distribution function for E:

$$p(E > E_T) = \int_{E_T}^{\infty} dE\; p(E) = \exp(-\bar{n}\tau)\exp\left(-\frac{E_T^2}{2\sigma_0^2}\right)$$

$$+\,\bar{n}\tau\,\exp(-\bar{n}\tau)\int_{\sigma_0^2}^{\infty} d\sigma^2\; p\left(\sigma_1^2 = \sigma^2 - \sigma_0^2\right)\exp\left(-\frac{E_T^2}{2\sigma^2}\right) \quad . \qquad (15)$$

To proceed further, it next is necessary to calculate $p(\sigma_1^2 = \sigma^2 - \sigma_0^2)$. This density function represents the effect on incident noise power at the receiving antenna, both of the spatial distribution of flashes about the antenna and of variability from flash to flash in the mean strength of the radiation from a flash. The spatial distribution of radiation sources within a flash, although of some interest (particularly the vertical extent because of the impact of source height on the

distance to the line-of-sight horizon), will not be addressed. Present data (e.g. Taylor[11] and Rustan[12]) are insufficient, and we cannot define this distribution with any confidence. A "representative" source height of 5 km will be used in the numerical examples that follow.

Few data have been found from which the variability in mean source strength from flash to flash could be inferred. However, in light of the large variation in incident noise power associated with the variability of source location, this limitation is unlikely to prove serious. The mean source strength averaged over all flashes is obtained from Figure 2. We assume that the total radiated energy is spread uniformly over the duration of a flash to obtain

$$\sigma_s^2 = \frac{2B}{\tau} S^2(f) \tag{16}$$

where σ_s^2 is the variance of the radiated field at unit distance; B is the receiver bandwidth; τ the mean flash duration; and S(f) the noise spectral amplitude at unit distance for the receiver frequency, f.

Given σ_s^2, σ_1^2 is known for a specific source location, once the propagation loss has been determined. Generally, we have

$$\sigma_1^2 = \sigma_s^2 \, g(\theta, \phi; h_s, h_r) \tag{17}$$

where the loss function, g, depends on the geocentric coordinates, (θ, ϕ), of the flash relative to the antenna, and on the respective heights, h_s and h_r of the source and the antenna above the earth's surface. This relationship is assumed to be known.

The loss function will also be taken to include a geometrical factor that specifies the loss associated with polarization and orientation mismatch between the incident noise field and the receiving antenna. For example, in the case of a vertically polarized monopole antenna, only the vertical component of the incident field is relevant, and $g(\theta, \phi; h_s, h_r)$ will include the factor $\sin^2(\theta_A)$, where θ_A is the zenith angle

of the source (flash) as seen from the antenna. In terms of the received noise power at the antenna terminals, this mismatch factor can be recognized as simply the receiving antenna pattern.

Unfortunately, the dependence of σ_1^2 on θ and ϕ is sufficiently complex for even a simple propagation model so that direct calculation of $p(\sigma_1^2)$ is awkward. This difficulty can, however, be circumvented by using the characteristic function for $p(\sigma_1^2)$, $M_{\sigma_1^2}(iv)$, to link the distribution of σ_1^2 to that of flash occurrence in the coordinate variables θ and ϕ. This last distribution is straightforward; the flash density for a given range, θ, is simply proportional to the area at that range.

We have then,

$$p(\sigma_1^2) = \frac{1}{2\pi} \int_{-\infty}^{\infty} dv \, M_{\sigma_1^2}(iv) \exp(-iv\sigma_1^2) \tag{18}$$

where the characteristic function, M, is defined[13] as the Fourier transform of the density function:

$$M_{\sigma_1^2}(iv) = \int_0^{\infty} d\sigma_1^2 \, p(\sigma_1^2) \exp(iv\sigma_1^2) \quad . \tag{19}$$

Equivalently,

$$M_{\sigma_1^2}(iv) = \int_0^{\pi} d\theta \int_0^{2\pi} d\phi \, p(\theta, \phi) \exp\left[iv\sigma_1^2(\theta, \phi)\right] \tag{20}$$

where $\sigma_1^2(\theta, \phi)$ is known by virtue of Eq. (17).

The probability, $p(\sigma_1^2 = \sigma^2 - \sigma_0^2)$, needed in Eqs. (14) and (15) follows simply by substitution of $\sigma^2 - \sigma_0^2$ for σ_1^2 in Eq. (18):

$$p(\sigma_1^2 = \sigma^2 - \sigma_0^2) = \frac{1}{2\pi} \int_{-\infty}^{\infty} dv \; M_{\sigma_1^2}(iv) \exp\left[-iv(\sigma^2 - \sigma_0^2)\right] \qquad (21)$$

$M_{\sigma_1^2}(iv)$ is unaffected by this substitution, being calculated generally in accordance with Eq. (20).

The probability-density function, $p(\theta, \phi)$, in Eq. (2) is given by

$$p(\theta, \phi)\, d\theta d\phi = \frac{r_e^2 \sin\theta \, d\theta \, d\phi}{A} \qquad (22)$$

where A is the area within which the flash is assumed to have occurred and r_e is the earth's radius. If attention is restricted to flashes within a limited range, such as those within line of sight of the receiving antenna, we obtain

$$A = 2\pi r_e^2 (1 - \cos\theta_m) \qquad (23)$$

where θ_m is the angular distance to a flash on the horizon; for a receiving antenna at ground height

$$\cos\theta_m = \frac{r_e}{r_e + h_s} \quad . \qquad (24)$$

The integration range for θ is correspondingly restricted in the calculation of $M_{\sigma_1^2}(iv)$ from Eq. (20); we have, insertings Eqs. (22) and (23),

$$M_{\sigma_1^2}(iv) = \frac{1}{2\pi(1 - \cos\theta_m)} \int_0^{\theta_m} d\theta \sin\theta \int_0^{2\pi} d\phi \exp\left[iv\sigma_1^2(\theta, \phi)\right] \qquad (25)$$

As an example of this procedure, we have calculated $p(\sigma_1^2)$ for the vertical electric component of the incident noise field at the earth's surface, using a simple line-of-sight propagation model. In this model, the noise power incident on the antenna from a flash varies inversely as the square of the distance, d, between the flash and the antenna. Equation (17), then, becomes, for this model,

$$\sigma_1^2 = \sigma_s^2 \left(\frac{r_s}{d}\right)^2 \sin^2 \theta_A \quad , \tag{26}$$

where r_s is the (unit) distance to which σ_s is referenced. The source-receiver geometry is illustrated in Figure 3, from which it can be seen

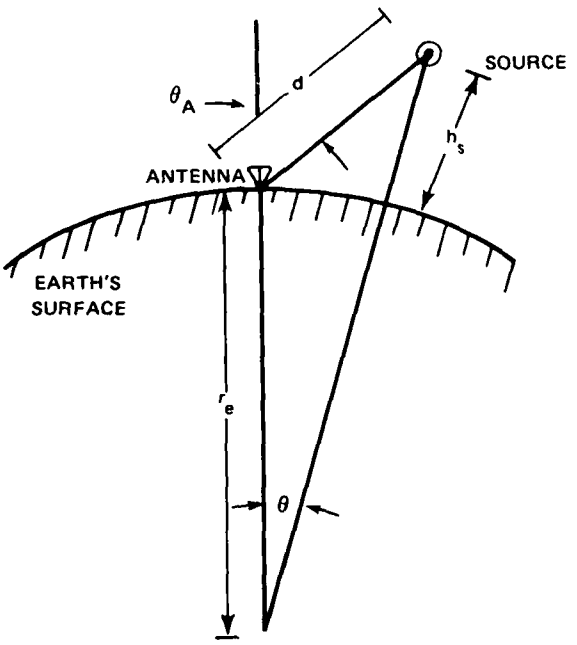

FIGURE 3 SOURCE-RECEIVER GEOMETRY
FOR LINE-OF-SIGHT PROPAGATION

that the source-receiver distance, d, is related to the angular distance, θ, by

$$d^2 = h_s^2 + 2r_e\,(r_e + h_s)(1 - \cos\theta) \quad , \tag{27}$$

where h_s is the source height. Additionally, the antenna pattern factor, $\sin\theta_A$, is related to θ by

$$\sin(\pi - \theta_A) = \frac{r_e + h_s}{d} \sin\theta \quad . \tag{28}$$

Insertion of these relationships into Eq. (26) gives

$$\sigma_1^2 = \sigma_s^2 \left[\frac{r_s\,(r_e + h_s)\sin\theta}{h^2 + 2\,r_e\,(r_e + h_s)(1 - \cos\theta)} \right]^2 \tag{29}$$

In this case, σ_1^2 is independent of ϕ; thus, the ϕ integration in Eq. (25) can be simply performed to obtain

$$M_{\sigma_1^2}(iv) = \frac{1}{1 - \cos\theta_m} \int_0^{\theta_m} d\theta \sin\theta \exp\left[iv\sigma_1^2(\theta)\right] \quad . \tag{30}$$

The variation of σ_1^2 as a function of θ given by Eq. (29) is shown in Figure 4 for a source height h_s = 5 km and strength $\sigma_s^2 = 1.6 \times 10^{-3}$ $(V/m)^2$. This value of σ_s^2 corresponds to a spectral amplitude S(f) = 0.02 Vs/m [Eq. (16)] for a frequency f = 10 MHz (Figure 2), a receiver bandwidth B = 1 Hz, and a mean flash duration τ = 0.5 s. The horizon in this example is at a surface distance $r_e\theta_m$ = 252 km.

The $\sigma_1^2(\theta)$ shown in Figure 4 yields the $p(\sigma_1^2 = \sigma^2 - \sigma_0^2)$ illustrated in Figure 5, when used in Eq. (21) with a background noise variance $\sigma_0^2 = 2.8 \times 10^{-20}$ $(V/m)^2$, corresponding [Eq. (4)] to a minimal background

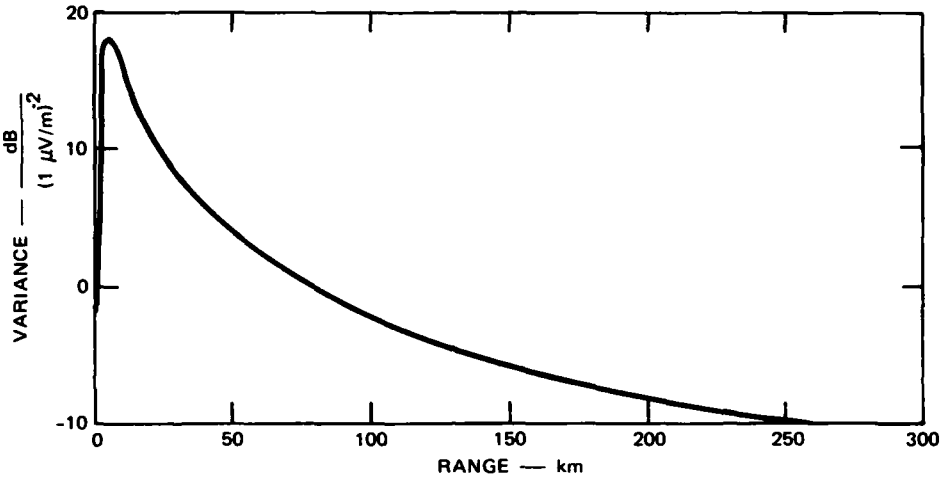

FIGURE 4 VARIATION WITH DISTANCE OF MEAN POWER RADIATED BY A SINGLE LIGHTNING FLASH

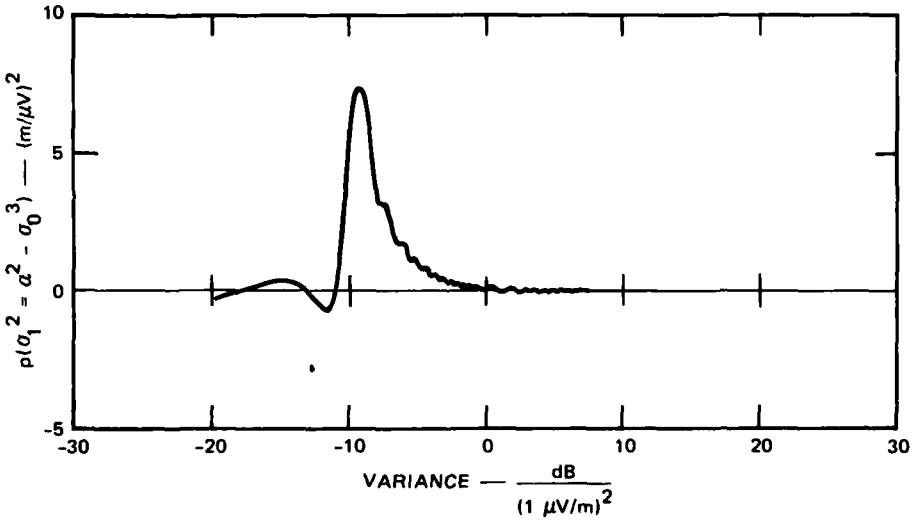

FIGURE 5 PROBABILITY DENSITY FUNCTION FOR MEAN RECEIVED POWER IN A ONE-Hz BANDWIDTH RADIATED BY A SINGLE FLASH

temperature T = 288 K. Over the range of σ^2 shown in Figure 5, $\sigma^2 >> \sigma_0^2$, and consequently $p(\sigma_1^2 = \sigma^2 - \sigma_0^2) \approx p(\sigma^2)$. The density function peaks at $\sigma^2 = 0.1\ (\mu V/m)^2$, which corresponds to the variance in the received noise field for a flash at the most likely range, namely the maximum range (cf. Figure 4). The oscillatory fine structure evident in Figure 5, which leads to some negative (and hence impossible) values for p at the small variances, is an artifact of the Fourier methods used in the calculation.

Use of the $p(\sigma_1^2)$, shown in Figure 5, to calculate p(E) and $P(E > E_T)$ from Eqs. (14) and (15) yields the results shown in Figures 6 and 7.

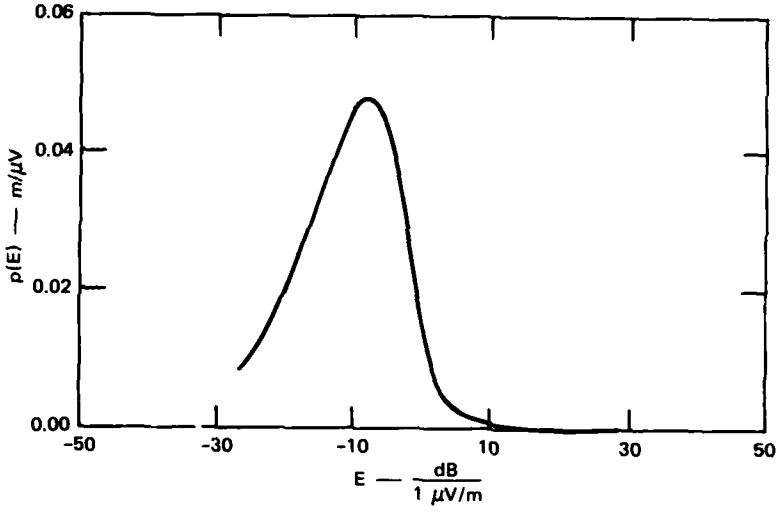

FIGURE 6 HIGH-AMPLITUDE PORTION OF PROBABILITY DENSITY FUNCTION FOR NOISE-ENVELOPE AMPLITUDE IN A ONE-Hz BANDWIDTH AT MODERATE LEVEL OF LOCAL THUNDERSTORM ACTIVITY

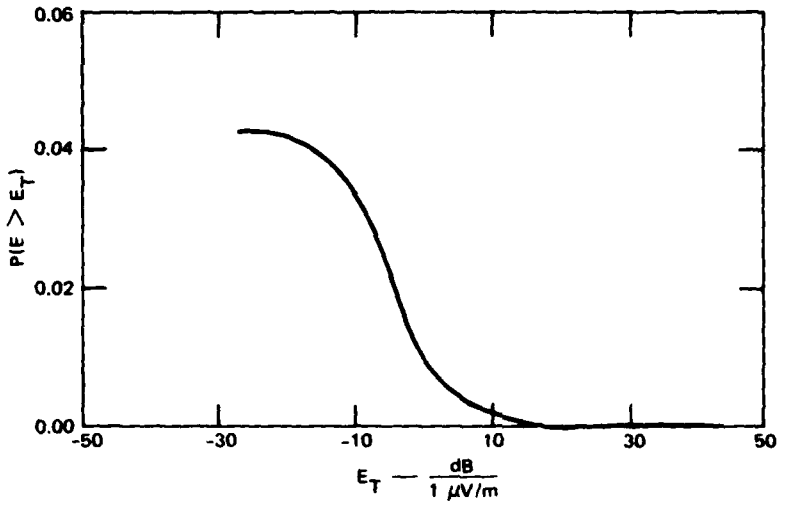

FIGURE 7 HIGH-AMPLITUDE PORTION OF PROBABILITY DISTRIBUTION FUNCTION FOR NOISE-ENVELOPE AMPLITUDE IN A ONE-Hz BANDWIDTH AT MODERATE LEVEL OF LOCAL THUNDERSTORM ACTIVITY

In this calculation, a mean flash rate of 1 per km^2 per month, corresponding to $\bar{n} = 0.08\ s^{-1}$ within line-of-sight range, was assumed. This flash density is representative of a region of moderate thunderstorm activity (5 thunderstorm days per month[2]). Again, only that portion of the total range of envelope amplitude has been shown in the figures for which the contribution of the noise produced by local lightning is significant. This contribution, given by the second terms of Eqs. (14) and (15), is approximately linear with $\bar{n}$ so long as $\bar{n}\tau$ remains small (for $\bar{n}\tau$ on the order of unity or greater, the effects of overlapping flashes also must be considered, as described in Section III.B).

The background contribution to the noise, given by the first terms of Eqs. (14) and (15), lies predominantely at much smaller values of E than those produced by close lightning, giving a peak in p(E) at E = σ_0(1.7×10^{-4} μV/m in this example). The probability density function

is bimodal, although the peak shown in Figure 6 is much smaller in magnitude than the one produced at smaller E by the background noise. The form of Eq. (15) further indicates that the integrated contribution to the envelope distribution from the background noise exceeds that from local flashes by a similar factor (i.e. in the ratio $\bar{n}_T$:1), as also shown by the leveling out of $P(E > E_T)$ for small E_T (but $>> \sigma_0$) in Figure 7.

B. Overlapping Flashes

Extension of the model presented in Section III.A to include the effects of overlapping flashes is not difficult in principle. We simply generalize Eq. (5) to a series in which each term corresponds to a given number of flashes, N, simultaneously in progress:

$$p(E) = \sum_{n=0}^{\infty} P(N)\ p(E|N) \quad . \tag{31}$$

The probability P(N) has already been determined (under the assumption of no correlation between flashes); it is given by Eq. (12).

The envelope probability density function given N flashes in progress, $p(E|N)$, is defined just as for N = 1, namely by Eq. (9)--except that $p(E|\text{flash}, \sigma^2)$ becomes $p(E|N, \sigma^2)$ and $p(\sigma^2)$ becomes $p(\sigma^2|N)$. Thus, we have

$$p(E|N) = \int d\sigma^2\ p(E|N, \sigma^2)\ p(\sigma^2|N) \quad . \tag{32}$$

Equation (10) also remains valid because we are dealing (as regards the field, not its envelope) with a sum of Gaussian random variables, which also is Gaussian. Now, however, σ^2 represents the sum of the σ_i^2 for N flashes plus σ_0^2 for the background:

$$\sigma^2 = \sum_{n=0}^{\infty} \sigma_i^2 \quad . \tag{33}$$

The variety of combinations of the σ_i^2 that can yield the same value for σ^2 is most readily dealt with through the characteristic functions for the $p(\sigma_i^2)$, defined by Eq. (19). Because σ^2 is formed as the sum of the statistically independent random variables σ_i^2, its characteristic function is[13] the product of those for the individual σ_i^2:

$$M_{\sigma^2}(iv) = \prod_{i=0}^{N} M_{\sigma_i^2}(iv) \tag{34}$$

With the exception of σ_0^2, the σ_i^2 are all drawn from the same population. Thus,

$$M_{\sigma^2}(iv) = M_{\sigma_0^2}(iv)\, M^N_{\sigma_1^2}(iv) \quad . \tag{35}$$

As previously, $M_{\sigma_1^2}(iv)$ can be readily calculated in terms of the geographic distribution of flashes, using Eq. (20).

The characteristic function $M_{\sigma_0^2}(iv)$ for the background component of the noise can be defined even though σ_0^2 has a fixed value and is not, in the conventional sense, a random variable. If we consider that a fixed σ_0^2 results as the limiting case when its distribution is narrowed to an infinitesimal width, however, we recognize $p(\sigma_0^2)$ as a delta function. Thus, from Eq. (19),

$$M_{\sigma_0^2}(iv) = \int_0^{\infty} d\sigma^2\, \delta(\sigma^2 - \sigma_0^2)\, \exp(iv\sigma^2) \tag{36a}$$

$$= \exp(iv\sigma_0^2) \quad . \tag{36b}$$

Fourier inversion of $M_{\sigma^2}(iv)$ now produces $p(\sigma^2|N)$:

$$p(\sigma^2|N) = \frac{1}{2\pi}\int_{-\infty}^{\infty} dv\, \exp\left[-iv(\sigma^2 - \sigma_0^2)\right] M^N_{\sigma_1^2}(iv) \tag{37}$$

[Equation (37) reduces, as it should, to Eq. (21) for N = 1.]

The use of Eq. (37) in Eq. (32), and this, in turn, with Eq. (12) in Eq. (31) yields

$$p(E) = \frac{\exp(-\bar{n}\tau)}{2\pi}\sum_{N=0}^{\infty}\frac{(\bar{n}\tau)^N}{N!}$$

$$\times \int_0^{\infty} d\sigma^2\, \frac{E}{\sigma^2}\exp(-E^2/2\sigma^2)\int_{-\infty}^{\infty} dv\, \exp\left[-iv(\sigma^2 - \sigma_0^2)\right] M^N_{\sigma_2^2}(iv) \quad . \tag{38}$$

If the summation in this expression is now brought within the integrals, there results

$$p(E) = \frac{\exp(-\bar{n}\tau)}{2\pi}\int_0^{\infty} d\sigma^2\, \frac{E}{\sigma^2}\exp(-E^2/2\sigma^2)$$

$$\times \int_{-\infty}^{\infty} dv\, \exp\left[-iv(\sigma^2 - \sigma_0^2)\right]\sum_{N=0}^{\infty}\frac{\left[\bar{n}\tau M_{\sigma_1^2}(iv)\right]^N}{N!} \quad . \tag{39}$$

in which the summation has been reduced to the Taylor series representation for the exponential function, whence

$$p(E) = \frac{1}{2\pi} \int_0^\infty d\sigma^2 \, \frac{E}{\sigma^2} \exp\left(-\frac{E^2}{2\sigma^2}\right)$$

$$\times \int_{-\infty}^{\infty} dv \, \exp\left[-iv(\sigma^2 - \sigma_0^2)\right] \exp\left\{\bar{n}\tau\left[M_{\sigma_1^2}(iv) - 1\right]\right\} \quad . \quad (40)$$

As previously, $p(E)$ can readily be integrated with respect to E to obtain $p(E > E_T)$:

$$p(E > E_T) = \frac{1}{2\pi} \int_0^\infty d\sigma^2 \, \exp\left(-\frac{E^2}{2\sigma^2}\right)$$

$$\times \int_{-\infty}^{\infty} dv \, \exp\left[-iv(\sigma^2 - \sigma_0^2)\right] \exp\left\{\bar{n}\tau\left[M_{\sigma_1^2}(iv) - 1\right]\right\} \quad . \quad (41)$$

The above approach does not depend strongly in its general development on the particular assumptions made concerning the nature of the noise radiated by an individual lightning flash. Furutsu and Ishida,[14] for example, have obtained somewhat comparable results employing a model in which non-uniform bursts of discrete noise pulses are folded with the receiver-impulse response to define the characteristics of the noise received from an individual flash. We have simplified this aspect of the model by assuming that the noise power is distributed uniformly, both temporally over the duration of the flash, and spectrally over the receiver pass band.

Furutsu and Ishida[14] do not, however, decompose, as we have, $p(E)$ into an integration over the joint distribution $p(E, \sigma^2)$. This step serves to isolate the influence on the noise of propagation loss, which

we have considered the dominant propagation effect, and allows it to be dealt with in some detail. Lacking effective computational means for handling the variation of propagation loss with range, Furutsu and Ishida[14] were constrained in application of their results to situations for which this loss was approximately the same for all sources.

Some preliminary calculations have been made employing Eqs. (40) and (41), but the results have not been completely satisfactory. The difficulties encountered are largely numerical, and appear to result, for the most part, from the embedding of the background noise contribution, whose characteristic function has constant amplitude out to large values of v, within the Fourier integrals. These difficulties should lessen as the mean number of flashes in progress at any time becomes large. This computational approach may thus have application in the joint treatment of noise arriving both by ground wave and by sky wave from a larger collection region.

For the treatment of overlapping noise flashes from within line-of-sight range alone, the mean flash rate remains low, even for highly active thunderstorm regions; thus, direct summation of the series in Eq. (39) is feasible. If this summation is performed following Fourier inversion of the characteristic function for each N on a term-by-term basis, the difficulties noted above are avoided.

This direct-summation approach was employed for a mean flash rate of 10 per km^2 per month, corresponding to an area of high thunderstorm activity (20 thunderstorm days per month[2]), to produce the results shown in Figures 8 through 10. The mean number of flashes in progress within line-of-sight range, is, in this case, appreciable; $\bar{n}\tau = 0.4$. With the exception of the increase by a factor of ten in mean flash rate, the parameter values used in this example are the same as those employed in Section III.A.

The shape of the density function, $p(\sigma^2)$, for the net variance, shown in Figure 8, is little changed (even at this flash density) from that for a single flash--illustrated in Figure 5. Careful comparison, however, reveals a shift in probability toward higher σ^2 values. This

change can also be found, on careful examination, in the envelope probability density function, p(E), Figure 9, and the distribution function, Figure 10.

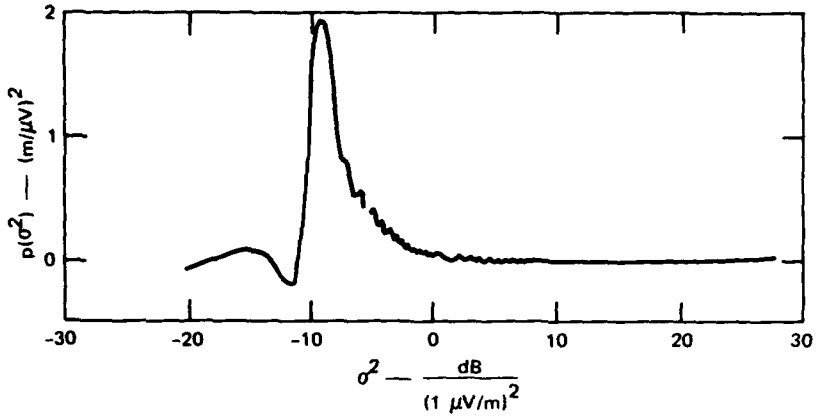

FIGURE 8 PROBABILITY DENSITY FUNCTION FOR MEAN RECEIVED POWER IN A ONE-Hz BANDWIDTH AT HIGH LEVEL OF LOCAL THUNDERSTORM ACTIVITY

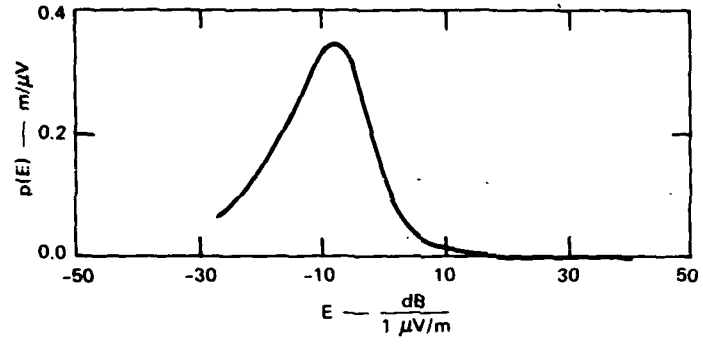

FIGURE 9 HIGH-AMPLITUDE PORTION OF PROBABILITY DENSITY FUNCTION FOR NOISE-ENVELOPE AMPLITUDE IN A ONE-Hz BANDWIDTH AT HIGH LEVEL OF LOCAL THUNDERSTORM ACTIVITY

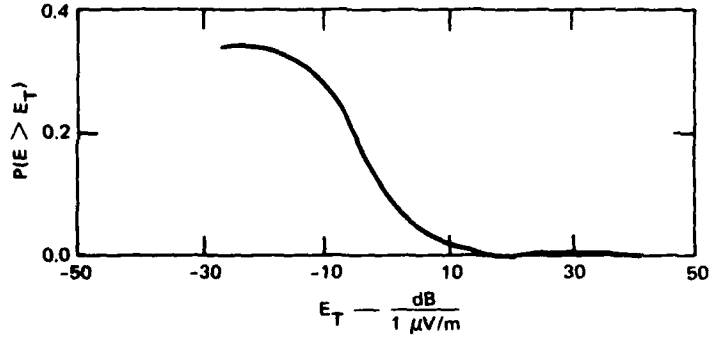

FIGURE 10 HIGH-AMPLITUDE PORTION OF PROBABILITY DISTRIBUTION FUNCTION FOR NOISE-ENVELOPE AMPLITUDE IN A ONE-Hz BANDWIDTH AT HIGH LEVEL OF LOCAL THUNDERSTORM ACTIVITY

REFERENCES

1. G. H. Price and G. Smith, "A Model of Natural HF Radio Noise in Severely Disturbed Propagation Environments," DNA 4930T, Topical Report for Period 17 November 1977-31 March 1979, Contract DNA001-77-C-0063, SRI Project 5978, SRI International, Menlo Park, CA (March 1979).

2. N. Cianos and E. T. Pierce, "A Ground-Lightning Environment for Engineering Usage," Technical Report 1, Contract L.S.-2817-A3, SRI Project 1834, Stanford Research Institute, Menlo Park, CA (August 1972).

3. WMO, "World Distribution of Thunderstorm Days--Part I," WMO/OMN No. 21, TP. 6, World Meteorological Organization, Geneva, Switzerland (1953).

4. CCIR, "World Distribution and Characteristics of Atmospheric Radio Noise," Report 322, International Telecommunications Union, Geneva, Switzerland (1964).

5. K. Davies, "Ionospheric Radio Propagation," National Bureau of Standards Monograph 80 (April 1, 1965).

6. A. F. Barghausen, et al., "Predicting Long-Term Operational Parameters of High-Frequency Sky-Wave Telecommunication Systems," Technical Report ERL 110-ITS 78, ESSA, Department of Commerce, Boulder, CO (May 1969).

7. J. R. Herman, "A Sensitive Technique for Detecting Late-Time Absorption Following High-Altitude Nuclear Explosions," Radio Science, Vol. 3, pp. 964-973 (1968).

8. G. N. Oetzel and E. T. Pierce, "The Radio Emissions From Close Lightning," Planetary Electrodynamics, Vol. 1, pp. 543-569 (Gordon and Breach, New York, 1969).

9. F. Horner, "Radio Noise From Thunderstorms," Advances in Radio Research, edited by J. A. Saxton, Vol. 2, pp. 121-204 (Academic Press, London, 1964).

10. W. B. Zavoli, "Observed Characteristics of Ionospherically Propagated HF Atmospherics from Normal and Severe Thunderstorms," Technical Report, IR&D Project 658D32-CIK, Stanford Research Institute, Menlo Park, CA (no date).

11. W. L. Taylor, "A VHF Technique for Space-Time Mapping of Lightning Discharge Processes," J. Geophys. Res., Vol. 83, pp. 3575-3584 (1978).

12. P. L. Rustan, M. A. Uman, D. G. Childers, W. H. Beasley, and C. L. Lennon, "Lightning Source Locations From VHF Radiation Data for a Flash at Kennedy Space Center," J. Geophys. Res., Vol. 85, pp. 4893-4903 (1980).

13. W. B. Davenport, Jr., and W. L. Root, An Introduction to the Theory of Random Signals and Noise, Sec. 4.3 (McGraw-Hill Book Company, Inc., New York, 1958).

14. K. Furutsu and T. Ishida, "On the Theory of Amplitude Distribution of Impulsive Radio Noise," J. Appl. Phys., Vol. 32, pp. 1206-1221 (1961).

DISTRIBUTION LIST

DEPARTMENT OF DEFENSE

Assistant Secretary of Defense
Comm, Cmd, Cont & Intell
ATTN: Dir of Intelligence Sys

Command & Control Technical Center
ATTN: C-312, R. Mason
ATTN: C-650, G. Jones
3 cy ATTN: C-650, W. Heidig

Defense Communications Agency
ATTN: Code 480, F. Dieter
ATTN: Code 480
ATTN: Code 205
ATTN: Code 101B

Defense Communications Engineer Center
ATTN: Code R123
ATTN: Code R410, N. Jones

Defense Intelligence Agency
ATTN: DT-1B
ATTN: DB-4C, E. O'Farrell
ATTN: DB, A. Wise
ATTN: Dir
ATTN: DC-7B

Defense Nuclear Agency
ATTN: NAFD
ATTN: NATD
ATTN: STNA
ATTN: RAEE
4 cy ATTN: TITL
5 cy ATTN: RAAE

Defense Technical Information Center
12 cy ATTN: DD

Field Command
Defense Nuclear Agency
ATTN: FCPR, J. McDaniel

Field Command
Defense Nuclear Agency
Livermore Branch
ATTN: FCPRL

Interservice Nuclear Weapons School
ATTN: TTV

Joint Chiefs of Staff
ATTN: C3S, Evaluation Office (HDOO)
ATTN: C3S

Joint Strat Tgt Planning Staff
ATTN: JLA
ATTN: JLTW-2

National Security Agency
ATTN: W-32, O. Bartlett
ATTN: R-52, J. Skillman
ATTN: B-3, F. Leonard

DEPARTMENT OF DEFENSE (Continued)

Under Secretary of Defense for Rsch & Engrg
ATTN: Strat & Theater Nuc Forces, B. Stephan
ATTN: Strategic & Space Sys (OS)

WWMCCS System Engineering Org
ATTN: R. Crawford

DEPARTMENT OF THE ARMY

Assistant Chief of Staff for Automation & Comm
Department of the Army
ATTN: DAMO-C4, P. Kenny

Atmospheric Sciences & Laboratory
U.S. Army Electronics R&D Command
ATTN: DELAS-EO, F. Niles

BMD Advanced Technology Center
Department of the Army
ATTN: ATC-T, M. Capps
ATTN: ATC-O, W. Davies

BMD Systems Command
Department of the Army
2 cy ATTN: BMDSC-HW

Deputy Chief of Staff for Ops & Plans
Department of the Army
ATTN: DAMO-RQC

Harry Diamond Laboratories
Department of the Army
ATTN: DELHD-NW-P
ATTN: DELHD-NW-R, R. Williams

U.S. Army Chemical School
ATTN: ATZN-CM-CS

U.S. Army Comm-Elec Engrg Instal Agency
ATTN: CCC-CED-CCO, W. Neuendorf
ATTN: CCC-EMEO-PED, G. Lane

U.S. Army Communications Command
ATTN: CC-OPS-W
ATTN: CC-OPS-WR, H. Wilson

U.S. Army Communications R&D Command
ATTN: DRDCO-COM-RY, W. Kesselman

U.S. Army Foreign Science & Tech Ctr
ATTN: DRXST-SD

U.S. Army Materiel Dev & Readiness Cmd
ATTN: DRCLDC, J. Bender

U.S. Army Nuclear & Chemical Agency
ATTN: Library

U.S. Army Satellite Comm Agency
ATTN: Document Control

DEPARTMENT OF THE ARMY (Continued)

U.S. Army TRADOC Sys Analysis Actvy
ATTN: ATAA-TCC, F. Payan, Jr
ATTN: ATAA-TDC
ATTN: ATAA-PL

USAMICOM
Department of the Army
ATTN: DRSMI-YSO, J. Gamble

DEPARTMENT OF THE NAVY

COMSPTEVFOR
Department of the Navy
ATTN: Code 605, R. Berg

Joint Cruise Missiles Project Ofc
Department of the Navy
ATTN: JCMG-707

Naval Air Development Center
ATTN: Code 6091, M. Setz

Naval Air Systems Command
ATTN: PMA 271

Naval Electronic Systems Command
ATTN: PME-117-2013, G. Burnhart
ATTN: PME-117-20
ATTN: Code 3101, T. Hughes
ATTN: PME 106-4, S. Kearney
ATTN: PME 106-13, T. Griffin
ATTN: PME 117-211, B. Kruger
ATTN: Code 501A

Naval Intelligence Support Ctr
ATTN: NISC-50

Naval Ocean Systems Center
ATTN: Code 5322, M. Paulson
ATTN: Code 532, J. Bickel
ATTN: Code 532, R. Pappert
3 cy ATTN: Code 5323, J. Ferguson

Naval Research Laboratory
ATTN: Code 7550, J. Davis
ATTN: Code 4780, S. Ossakow
ATTN: Code 4187
ATTN: Code 7950, J. Goodman
ATTN: Code 4700, T. Coffey
ATTN: Code 7500, B. Wald

Naval Space Surveillance System
ATTN: J. Burton

Naval Surface Weapons Center
ATTN: Code F31

Naval Telecommunications Command
ATTN: Code 341

Office of Naval Research
ATTN: Code 465
ATTN: Code 420
ATTN: Code 421

DEPARTMENT OF THE NAVY (Continued)

Office of the Chief of Naval Operations
ATTN: OP 981N
ATTN: OP 941D
ATTN: NOP 65

Strategic Systems Project Office
Department of the Navy
ATTN: NSP-2141
ATTN: NPS-2722, F. Wimberly
ATTN: NSP-43

DEPARTMENT OF THE AIR FORCE

Aerospace Defense Command
Department of the Air Force
ATTN: DC, T. Long

Air Force Geophysics Laboratory
ATTN: OPR, H. Gardiner
ATTN: OPR-1
ATTN: LKB, K. Champion
ATTN: OPR, A. Stair
ATTN: S. Basu
ATTN: PHP
ATTN: PHI, J. Buchau
ATTN: R. Thompson

Air Force Weapons Laboratory
Air Force Systems Command
ATTN: SUL
ATTN: NTYC
ATTN: NTN

Air Force Wright Aeronautical Lab/AAAD
ATTN: A. Johnson
ATTN: W. Hunt

Air Logistics Command
Department of the Air Force
ATTN: OO-ALC/MM

Air University Library
Department of the Air Force
ATTN: AUL-LSE

Headquarters
Air Weather Service, MAC
Department of the Air Force
ATTN: DNXP, R. Babcock

Assistant Chief of Staff
Studies & Analyses
Department of the Air Force
ATTN: AF/SASC, W. Krauss
ATTN: AF/SASC, C. Rightmeyer

Ballistic Missile Office/DAA
Air Force Systems Command
ATTN: ENSN, J. Allen

Headquarters
Electronic Systems Division
Department of the Air Force
ATTN: DCKC, J. Clark

DEPARTMENT OF THE AIR FORCE (Continued)

Deputy Chief of Staff
Operations Plans and Readiness
Department of the Air Force
ATTN: AFXOXFD
ATTN: AFXOKT
ATTN: AFXOKS
ATTN: AFXOKCD

Deputy Chief of Staff
Research, Development, & Acq
Department of the Air Force
ATTN: AFRDS
ATTN: AFRDSP
ATTN: AFRDSS

Headquarters
Electronic Systems Division
Department of the Air Force
ATTN: OCT-4, J. Deas

Headquarters
Electronic Systems Division
Department of the Air Force
ATTN: YSEA
ATTN: YSM, J. Kobelski

Foreign Technology Division
Air Force Systems Command
ATTN: TQTD, B. Ballard
ATTN: NIIS Library

Rome Air Development Center
Air Force Systems Command
ATTN: TSLD
ATTN: OCS, V. Coyne

Rome Air Development Center
Air Force Systems Command
ATTN: EEP

Space Division
Department of the Air Force
ATTN: YGJB, W. Mercer

Space Division
Department of the Air Force
ATTN: YKA, D. Bolin
ATTN: YKA, C. Kennedy

Strategic Air Command
Department of the Air Force
ATTN: XPFS
ATTN: DCXT
ATTN: NRT
ATTN: DCXR, T. Jorgensen
ATTN: DCX

OTHER GOVERNMENT AGENCIES

Central Intelligence Agency
ATTN: OSWR/NED

Department of Commerce
National Bureau of Standards
ATTN: Sec Ofc for R. Moore

OTHER GOVERNMENT AGENCIES (Continued)

Department of Commerce
National Oceanic & Atmospheric Admin
Environmental Research Laboratories
ATTN: R. Grubb

Institute for Telecommunications Sciences
National Telecommunications & Info Admin
ATTN: L. Berry
ATTN: W. Utlaut
ATTN: A. Jean

DEPARTMENT OF ENERGY CONTRACTORS

EG&G, Inc
Los Alamos Division
ATTN: J. Colvin
ATTN: D. Wright

Lawrence Livermore National Lab
ATTN: Technical Info Dept Library
ATTN: L-31, R. Hager
ATTN: L-389, R. Ott

Los Alamos National Laboratory
ATTN: T. Kunkle, ESS-5
ATTN: C. Westervelt
ATTN: MS 670, J. Hopkins
ATTN: P. Keaton
ATTN: D. Simons
ATTN: MS 664, J. Zinn

Sandia National Laboratories
Livermore Laboratory
ATTN: B. Murphey
ATTN: T. Cook

Sandia National Lab
ATTN: Space Project Div
ATTN: Org 1250, W. Brown
ATTN: D. Dahlgren
ATTN: 3141
ATTN: Org 4241, T. Wright
ATTN: D. Thornbrough

DEPARTMENT OF DEFENSE CONTRACTORS

Aerospace Corp
ATTN: N. Stockwell
ATTN: D. Olsen
ATTN: J. Straus
ATTN: S. Bower
ATTN: I. Garfunkel
ATTN: V. Josephson
ATTN: T. Salmi
ATTN: R. Slaughter

Analytical Systems Engineering Corp
ATTN: Radio Sciences

Analytical Systems Engineering Corp
ATTN: Security

Barry Research Corporation
ATTN: J. McLaughlin

DEPARTMENT OF DEFENSE CONTRACTORS (Continued)

BDM Corp
ATTN: T. Neighbors
ATTN: L. Jacobs

Berkeley Research Associates, Inc
ATTN: J. Workman

Betac
ATTN: J. Hirsch

Boeing Co
ATTN: S. Tashird
ATTN: G. Hall
ATTN: M/S 42-33, J. Kennedy

Booz-Allen & Hamilton, Inc
ATTN: B. Wilkinson

University of California at San Diego
ATTN: H. Booker

Charles Stark Draper Lab, Inc
ATTN: J. Gilmore
ATTN: D. Cox

Computer Sciences Corp
ATTN: F. Eisenbarth

Comsat Labs
ATTN: G. Hyde
ATTN: D. Fang

Cornell University
ATTN: D. Farley, Jr
ATTN: M. Kelly

E-Systems, Inc
ATTN: R. Berezdivin

Electrospace Systems, Inc
ATTN: H. Logston

ESL, Inc
ATTN: J. Marshall
ATTN: R. Ibaraki
ATTN: R. Heckman
ATTN: J. Lehman
ATTN: E. Tsui

General Electric Co
ATTN: A. Harcar

General Electric Co
ATTN: C. Zierdt
ATTN: A. Steinmayer

General Electric Co
ATTN: F. Reibert

General Electric Co
ATTN: G. Millman

General Research Corp
ATTN: J. Ise, Jr
ATTN: J. Garbarino

DEPARTMENT OF DEFENSE CONTRACTORS (Continued)

Harris Corp
ATTN: E. Knick

Horizons Technology, Inc
ATTN: R. Kruger

HSS, Inc
ATTN: D. Hansen

IBM Corp
ATTN: H. Ulander

University of Illinois
ATTN: Security Supervisor for K. Yeh

Institute for Defense Analyses
ATTN: E. Bauer
ATTN: H. Gates
ATTN: H. Wolfhard
ATTN: J. Aein

International Tel & Telegraph Corp
ATTN: W. Rice
ATTN: Technical Library

JAYCOR
ATTN: J. Sperling

JAYCOR
ATTN: J. Doncarlos

Johns Hopkins University
ATTN: T. Potemra
ATTN: J. Phillips
ATTN: T. Evans
ATTN: J. Newland
ATTN: P. Komiske

Kaman Tempo
ATTN: W. Knapp
ATTN: T. Stephens
ATTN: DASIAC
ATTN: W. McNamara

Linkabit Corp
ATTN: I. Jacobs

Litton Systems, Inc
ATTN: R. Grasty

Lockheed Missiles & Space Co, Inc
ATTN: W. Imhof
ATTN: R. Johnson
ATTN: M. Walt

Lockheed Missiles & Space Co, Inc
ATTN: Dept 60-12
ATTN: C. Old/Dept 68-21
ATTN: D. Churchill/Dept 81-11

M.I.T. Lincoln Lab
ATTN: D. Towle

Magnavox Govt & Indus Electronics Co
ATTN: G. White

DEPARTMENT OF DEFENSE CONTRACTORS (Continued)

Martin Marietta Corp
ATTN: R. Hefiner

McDonnell Douglas Corp
ATTN: H. Spitzer
ATTN: R. Halprin
ATTN: W. Olson

Meteor Communications Consultants
ATTN: R. Leader

Mission Research Corp
ATTN: R. Hendrick
ATTN: Tech Library
ATTN: D. Sappenfield
ATTN: F. Fajen
ATTN: S. Gutsche
ATTN: R. Kilb
ATTN: R. Bogusch

Mitre Corp
ATTN: C. Callahan
ATTN: B. Adams
ATTN: A. Kymmel
ATTN: G. Harding

Mitre Corp
ATTN: M. Horrocks
ATTN: W. Foster
ATTN: W. Hall
ATTN: J. Wheeler

Pacific-Sierra Research Corp
ATTN: F. Thomas
ATTN: E. Field, Jr
ATTN: H. Brode

Pennsylvania State University
ATTN: Ionospheric Research Lab

Photometrics, Inc
ATTN: I. Kofsky

Physical Dynamics, Inc
ATTN: E. Fremouw

Physical Research, Inc
ATTN: R. Deliberis

R & D Associates
ATTN: W. Wright
ATTN: R. Turco
ATTN: M. Gantsweg
ATTN: R. Lelevier
ATTN: W. Karzas
ATTN: B. Gabbard
ATTN: H. Ory
ATTN: F. Gilmore
ATTN: C. Greifinger
ATTN: P. Haas

R & D Associates
ATTN: B. Yoon

Rand Corp
ATTN: E. Bedrozian
ATTN: C. Crain

DEPARTMENT OF DEFENSE CONTRACTORS (Continued)

Riverside Research Institute
ATTN: V. Trapani

Rockwell International Corp
ATTN: R. Buckner

Rockwell International Corp
ATTN: S. Quilici

Santa Fe Corp
ATTN: D. Paolucci

Science Applications, Inc
ATTN: C. Smith
ATTN: D. Hamlin
ATTN: E. Straker
ATTN: L. Linson

Science Applications, Inc
ATTN: SZ

Science Applications, Inc
ATTN: J. Cockayne

SRI International
ATTN: G. Smith
ATTN: M. Baron
ATTN: R. Livingston
ATTN: C. Rino
ATTN: W. Jaye
ATTN: R. Leadabrand
ATTN: W. Chesnut
ATTN: D. Neilson
ATTN: J. Petrickes
ATTN: R. Tsunoda
ATTN: A. Burns
4 cy ATTN: G. Price
4 cy ATTN: V. Hatfield

Sylvania Systems Group
ATTN: I. Kohlberg
ATTN: J. Concordia
ATTN: R. Steinhoff

Technology International Corp
ATTN: W. Boquist

Tri-Com, Inc
ATTN: D. Murray

TRW Electronics & Defense Sector
ATTN: R. Plebuch
ATTN: D. Dee

Utah State University
ATTN: J. Dupnik
ATTN: L. Jensen
ATTN: K. Baker

Visidyne, Inc
ATTN: J. Carpenter
ATTN: C. Humphrey


FIL
07